

Supplementary Information (SI) to:

Development of Magnetocaloric Microstructures from Equiatomic FeRh Nanoparticles through Laser Sintering

Shabbir Tahir¹, Joachim Landers², Soma Salamon², David Koch³, Carlos Doñate-Buendía¹, Anna R. Ziefuß⁴, Heiko Wende², and Bilal Gökce^{1*},

¹ Chair of Materials Science and Additive Manufacturing, University of Wuppertal, Gaußstr. 20, 42119 Wuppertal, Germany

² Faculty of Physics and Center for Nanointegration Duisburg-Essen (CENIDE), University of Duisburg-Essen, Lotharstr. 1, 47057 Duisburg, Germany

³ Institute of Materials Science, Technical University of Darmstadt, Darmstadt 64287, Alarich-Weiss-Str. 2, Germany

⁴ Technical Chemistry I and Center for Nanointegration Duisburg-Essen (CENIDE), University of Duisburg-Essen, Universitätsstr. 7, 45141 Essen, Germany

* Corresponding author: goekce@uni-wuppertal.de; Tel.: +49-202-439-5385

1. Synthesis of FeRh nanoparticles by pulsed laser ablation of ~~FeRh target~~ in ethanol.

The scanning electron microscope imaging shows ~~that~~ the formation of spherical nanoparticles of distinct sizes (Inset Fig. S1). The size distribution gives an overview of the maximum ferret diameter of 558 nanoparticles. It has to be noted that the particles less than 2 nm were difficult to resolve, and only clearly visible, non-agglomerated particles were considered. The distribution ~~shows higher~~ size fraction of smaller nanoparticles (< 10 nm) with a peak maximum of 6.9 nm; and ~~were~~ fitted using lognormal distribution. The Polydispersity index (PDI) ~~give~~ an overall impression of dispersity and since the PDI is higher than 0.3, the distribution is polydisperse.

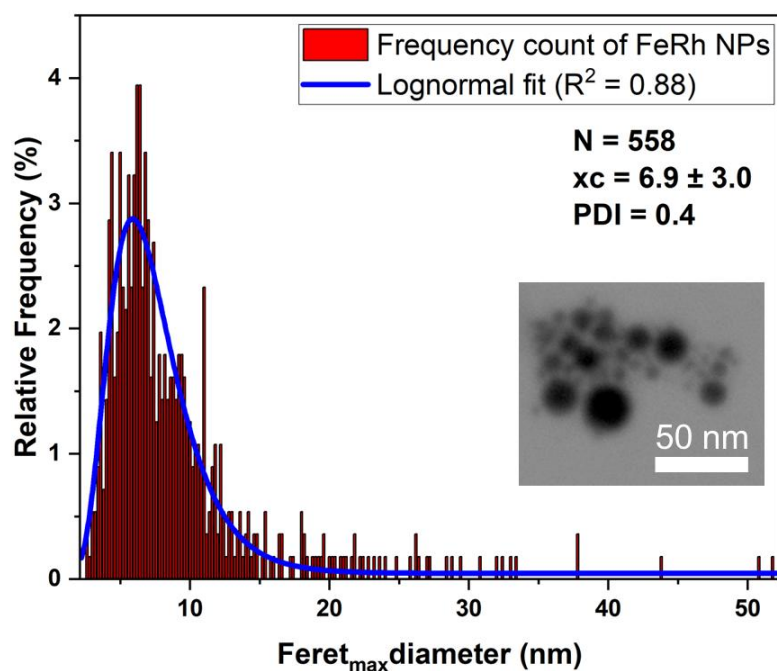


Figure S1: Particle size distribution as extracted from the SEM images of homogeneously dispersed FeRh nanoparticles (558 particles were counted).

2. Mass approximation of laser sintered FeRh ink using reflectance spectroscopy.

Reflectance spectroscopy is a technique commonly used for characterizing both powder and thin films. In this method, light from a source is transmitted through an optical fibre to a probe and directed onto the substrate of interest. The reflected light is then captured by the probe and analyzed using a spectrometer. This principle is depicted in Fig. S2. The amount of reflection depends on several factors including the coating material, thickness of the coating, and substrate. To ensure consistent background measurements, the substrate is positioned on a white holder during analysis. As a rule, the denser the coating, the lower the level of reflection observed from the film. To avoid any reflection from the glass, the ink deposition and sintering was performed on the white glass-ceramic substrate, which has similar thermal conductivity and thermal diffusivity as glass, to avoid any differences in sintering characteristics. Initially, the calibration was performed, in which ink containing FeRh NPs of different concentration (i.e., known mass) was deposited on a defined substrate area of 25 x 15 mm and sintered at the laser fluence of 41 J/cm². The reflectance at various laser fluence was measured between the wavelength of 200 to 1150 nm (Fig. S3a). The reflectance at various wavelengths between 600 nm and 900 nm was measured for each fluence (Fig. S3b). The results indicated a linear increase in reflectance with increasing fluence. The observed increase is attributed to the reduction in nanoparticle ink concentration caused by the ablation process. The decrease in concentration leads to a thinner coating layer, causing more reflection from the white glass-ceramic

substrate. These linear relationships can be employed to determine the reflectance of sintered films at different laser fluences, provided that the experimental procedure remains consistent.

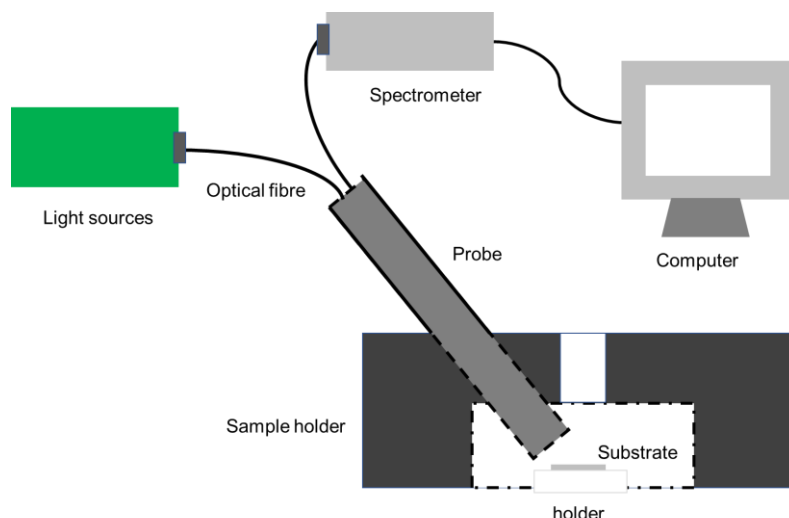


Figure S2. Schematic representation of mobile UV-VIS reflectance spectrometer used to measure the reflectance of sintered FeRh dispersed ink.

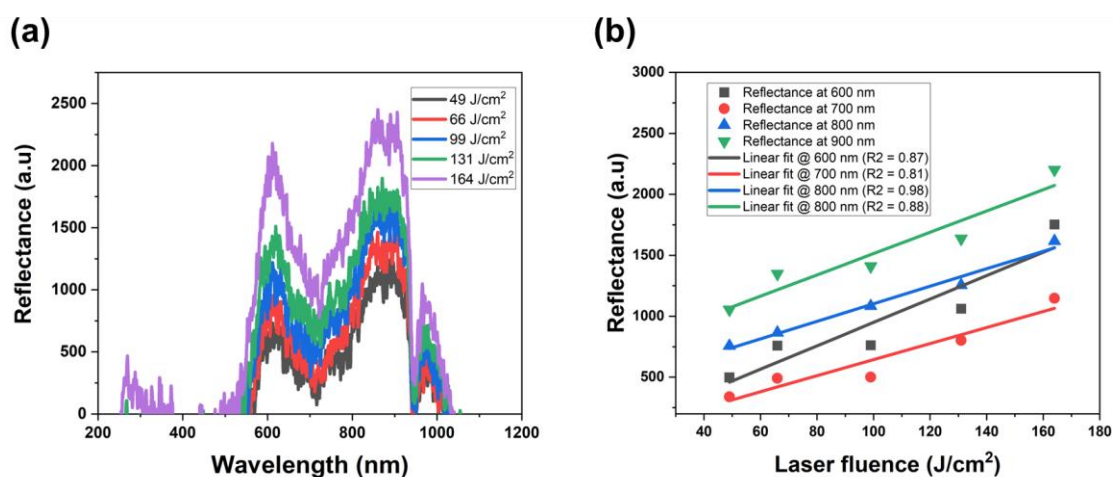


Figure S3. (a) Reflectance obtained from UV-VIS reflectometer at wavelengths between 200 to 1150 nm for the FeRh inks of different mass dispersed on the glass-ceramic substrate and sintered at fluences ranging from 49 - 164 J/cm^2 provided that the surface area of dispersion was kept constant. **(b)** The dependence of reflectance on the laser fluence for the wavelengths between 600 – 900 nm, along with the line of best fits for each fluence.

3. Temperature-dependent magnetization measurements

The distribution of phase transition temperatures of laser-sintered samples from the low temperature antiferromagnetic to the high-temperature ferromagnetic state was evaluated as follows: For the sample laser sintered at a fluence of 246 J/cm^2 we recorded the magnetization between 150 K and 700 K at 0.1 T as shown in Fig. S4. One has to keep in mind that $M(T)$ data displayed here still

contains an underlying magnetization signal originating from the glass substrate the FeRh nanoparticles were deposited on. Still, one can clearly discern the increase in magnetization slowly beginning at ca. 200 K, marking the onset of the AFM-to-FM phase transition. Possible reasons for the broadening of the phase transition as compared to bulk FeRh samples can be due to minor variation in stoichiometry and structural defects in NPs during their production by LAL. It is reasonable to assume the peak at ca. 460 K to represent the highest phase transition temperatures in our sample, above which all FeRh can be considered as ferromagnetic, with $M(T)$ decreasing again when going to even higher temperatures, approaching T_C .

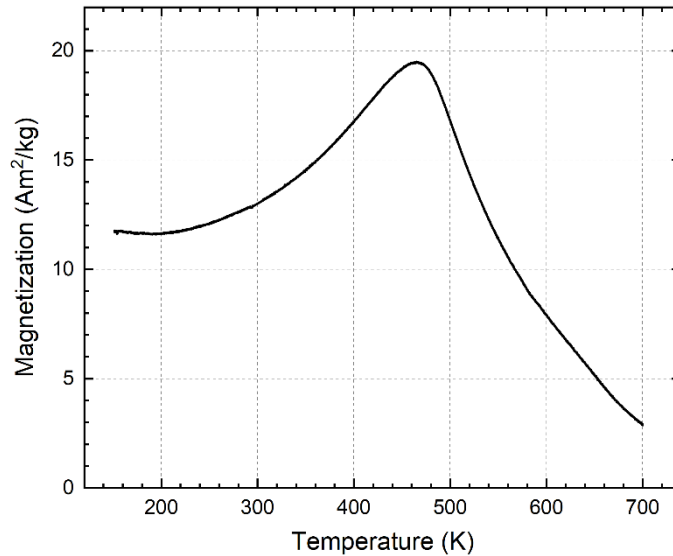


Figure S4. Temperature dependent magnetization $M(T)$ recorded between 700 K and 150 K upon cooling in an applied magnetic field of 0.1 T.

4. Estimation of entropy change ΔS_{mag}

As already mentioned in the main text, the preparation of a thin layer of laser-sintered FeRh nanoparticles on a glass substrate results in a marginal magnetization superimposed by a considerable dia- and paramagnetic substrate contribution. It is therefore very challenging to obtain precise values for FeRh magnetization and magnetocaloric effect, especially in the low-temperature region, where the miniscule field-induced increase in magnetization is still almost linear. To enable at least a rough assessment of magnetocaloric performance of the produced laser-sintered nanostructures, the contribution of the AFM-FM phase transition to the magnetic entropy change ΔS_{mag} was estimated as shown in fig. S5 for two pieces of the sample laser sintered at a fluence of 246 J/cm² to 3 - 3.5 J/kg·K between 0 and 9 T. Here, we followed the method described by Pecharsky et al. to extract ΔS_{mag} from a set of $M(H)$ curves recorded at different temperatures.¹

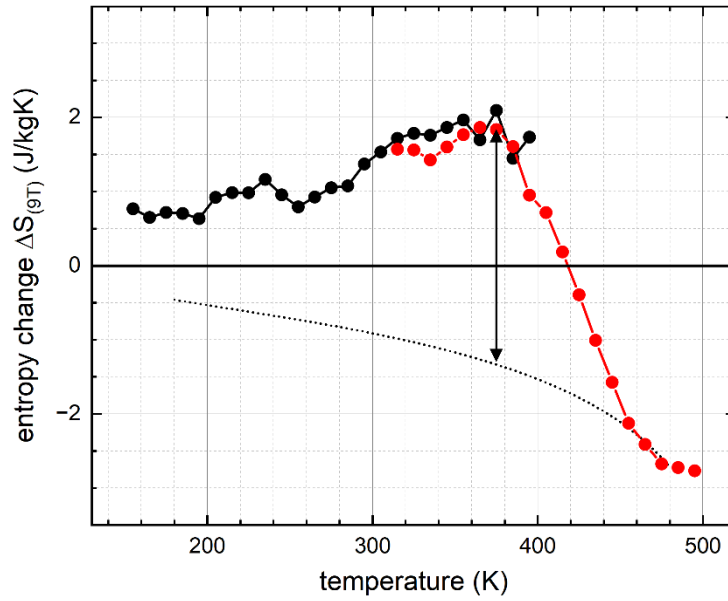


Figure S5. Entropy change determined following the method by Pecharsky et al. between 0 T and 9 T for two pieces of a sample laser sintered at a fluence of 246 J/cm^2 .¹ Black data points were recorded between 150 K and 400 K using the large bore VSM option of a PPMS DynaCool, while red data points denote measurements recorded between 300 K and 500 K for a second, smaller piece of the same sample mounted on a different VSM sample holder type for high temperature measurements. The dotted line is a guide to the eye representing extrapolated values of ΔS_{mag} in the absence of the AFM-FM phase transition based on the high-temperature data. The arrow marks the maximum ΔS_{mag} at ca. 380 K originating from the phase transition, amounting to ca. 3 - 3.5 J/kg·K between 0 T and 9 T.

References

1. Pecharsky, V. K.; Gschneidner, K. A., Magnetocaloric effect from indirect measurements: Magnetization and heat capacity. *J. Appl. Phys.* **1999**, 86(1), 565-575